· Article · Advances in Polar Science
doi: 10.13679/j.advps.2018.4.00243 December 2018 Vol. 29 No. 4: 243-253

Records in palaeo-notch sediment: changes in palaeo-productivity and their link to climate change from Svalbard

YANG Zhongkang[1,2], WANG Yuhong[1,2] & SUN Liguang[1,2]*

[1] Anhui Province Key Laboratory of Polar Environment and Global Change, School of Earth and Space Sciences, University of Science and Technology of China, Hefei 230026, China;
[2] Institute of Polar Environment, School of Earth and Space Sciences, University of Science and Technology of China, Hefei 230026, China

Received 18 July 2018; accepted 4 December 2018

Abstract Palaeo-notch sediment, accumulated in lacustrine environment, is a reliable proxy material for palaeoclimatic and palaeoenvironmental research. In this study, we collected a palaeo-notch sediment profile from the Blomstrandhalvøya, used multiple geochemical proxies to reconstruct palaleoproductivity variations, and investigated their link to climatic records from surrounding regions. C/N atomic ratios and carbon isotope indicate that organic matter in the sediment is mainly derived from lacustrine algae. Toward the surface sediment, the TOC, TN, P contents and the reconstructed palaeoproductivity show remarkable fluctuations with several peaks and troughs, opposite to the variation trend of the $CaCO_3$ contents. Changes in the reconstructed palaeoproductivity are in good agreement with palaeoclimatic records from the surrounding regions, and three interruptions are likely linked to the well-known cooling periods around 1900 BP, 2800 BP and 4200 BP. Thus palaeoproductivity variations on the Blomstrandhalvøya are mainly driven by climate changes; palaeoproductivity increase during warmer periods, and vice versa. This study will help the research of Arctic lake ecosystem and its response to climate change.

Keywords **palaeo-notch sediment, geochemical analysis, palaleoproductivity, climate change, Svalbard**

Citation: Yang Z K, Wang Y H, Sun L G. Records in palaeo-notch sediment: changes in palaeoproductivity and their link to climate change from Svalbard. Adv Polar Sci, 2018, 29(4): 243-253, doi: 10.16379/j.advps.4.00243

1 Introduction

The Arctic is undergoing profound climate changes in recent decades (Cohen et al., 2014; Jiang et al., 2011), and climate model results (Holland et al., 2006) show that rapid climate warming, known as “polar amplification” phenomenon, will continue in the future (Røthe et al., 2015). The available instrumental climate records in the Arctic are sparsely distributed and of short-time span; therefore, many proxy climate records have been reconstructed to study the natural climate changes in the Arctic region (Yang et al., 2017; Balascio et al., 2015; Gajewski, 2015; Røthe et al., 2015; Miller et al., 2010; Bond et al., 2001).

Svalbard is a high Arctic Archipelago, and it is very sensitive to climate change. Although the climate changes in Svalbard have been well studied (Røthe et al., 2015; van der Bilt et al., 2015), to the best of our knowledge, research on palaeoproductivity using lacustrine sediment have rarely been reported in Svalbard. The organic matter in lacustrine sediments mainly consists of detritus from algae in the lake or terrestrial plants in the drainage basin (Kołaczek et al.,

* Corresponding author, E-mail: slg@ustc.edu.cn

2015; Meyers and Ishiwatari, 1993). When the vegetation in or around the lakes flourishes, the amount of organic matter in lacustrine records rises correspondingly. Organic matter is an important part of the lacustrine sediment, and it provides significant information about palaeoenvironmental variations and the history of climate change (Kołaczek et al., 2015; Vreca and Muri, 2006).

Lack of studies on lacustrine palaeoproductivity in Svalbard is likely due to lack of good study materials, especially in Spitsbergen. Glaciers during the Little Ice Age in western Spitsbergen were the largest during the Holocene (Mangerud and Landvik, 2007) and destroyed large quantities of lacustrine sediment sequences. Sun et al. (2005) identified palaeo-notch sediments as lacustrine sediments and proposed that palaeo-notches sediments are reliable proxy materials for palaeoclimate and palaeoenvironment research in Antarctica.

In our previous work, we reconstructed mid- to late Holocene climate change records (Yang et al., 2018) and this study is a more in-depth study of our earlier work. In the present study, we collected a well-preserved palaeo-notch sediment sequence in Svalbard. We analyzed the geochemical characteristics of organic matter in the sediment profile, and the C/N atomic ratios and stable carbon isotopes indicate that organic matter is mainly derived from lake algae. From this sediment profile, we reconstructed the history of palaeoproductivity variations, and discussed its responses to climate change.

2 Study area

The Svalbard archipelago (74°–81°N; 10°–35°E) has a total land area of approximately 63000 km^2 and two-thirds of the land is permanently covered by ice and glaciers, which are especially extensive in north-eastern part (Jiang et al., 2011; Birks et al., 2004). During the Last Glacial Maximum, Svalbard was totally covered by the Late Weichselian Barents ice sheet (Landvik et al., 1998). The margin of Late Weichselian ice retreated to the western coast of Svalbard around 13000–12000 BP and the islands gradually appeared (Forman et al., 2004; Mangerud et al., 1992). Although the Svalbard archipelago was located entirely in the High Arctic region, there exists a great diversity of vegetation in Svalbard including 742 lichen species, 373 bryophyte species, and 173 vascular plant species (Zhang et al., 2015).

Blomstrandhalvøya is located in the middle of Kongsfjorden, close to the NW coast and facing the settlement of Ny-Ålesund. It is ~ 5 km long and < 4 km wide with an area of 16.4 km^2. The bedrock of the island mainly consists of medium-to-high-grade metamorphic marble (Proterozoic age) with a very thin surface weathering, while the unmetamorphosed redbeds sediments (Devonian) are present only in scattered remnants of a more widespread blanket of Devonian sediments (Miccadei et al., 2016).

The samples were collected on the Blomstrandhalvøya, about 5 km north of Ny-Ålesund in the Svalbard archipelago (Figure 1). The mean temperature in Ny-Ålesund between 1969 and 2013 was −4.2℃, while the mean temperature from October to February and from March to June was −9.2℃ and −1.4℃, respectively. The mean annual precipitation was 415.5 mm, most of which is accumulated in the early snow season (López-Moreno et al., 2016).

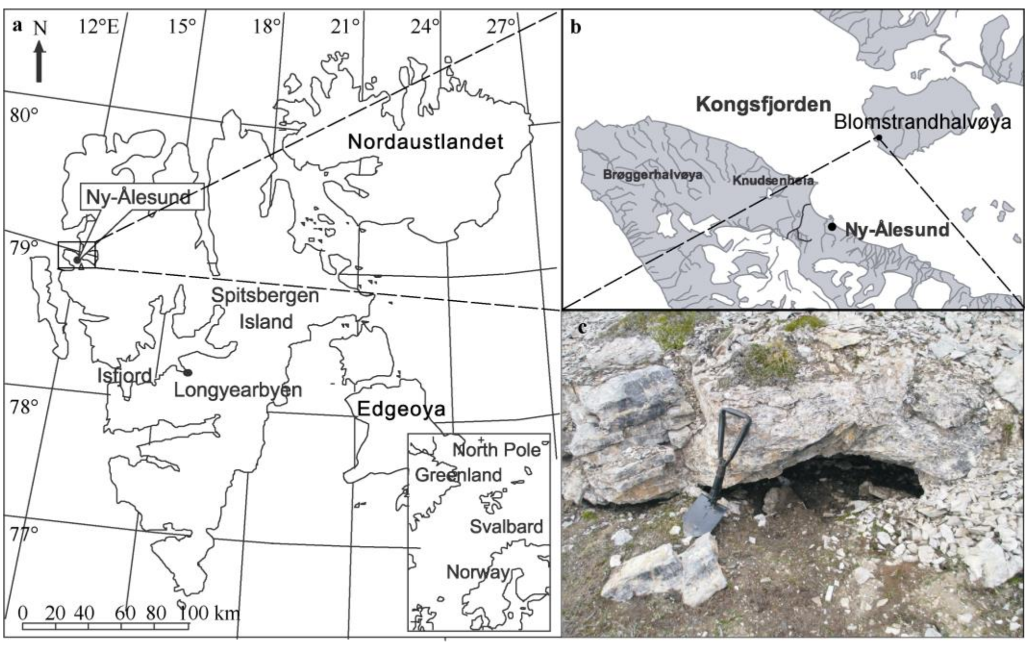

Figure 1 Map of studied area and sampling site. **a**, Location of Svalbard Islands; **b**, Location of Ny-Ålesund; **c**, Location of sampling site.

3 Materials and methods

3.1 Sample collection

A 36-cm-long undisturbed palaeo-notch sediment profile was excavated using a small shovel on the Blomstrandhalvøya (78°57′46" N, 12°02′10" E) during the China Arctic Expedition in 2014. The palaeo-notch is located in the southwestern side of Blomstrandhalvøya, about 5 km north of the Yellow River Station of China. The palaeo-notch was discovered in the marine terrace of Blomstrandhalvøya, about 8 m above sea level, it opens towards the southwest, it is approximately 80 cm wide, 50 cm deep and 30 cm high and its configuration is very similar to that of the palaeo-notch found in Antarctica (Sun et al., 2005). Based on the field observation and existing results, this palaeo-notch is likely formed by ocean wave before rising to the terrace (Yuan et al., 2010; Sun et al., 2005). The detailed description and formation process of the palaeo-notch LDP was illustrated in our previous research (Yang et al., 2018). The sediment profile LDP is a brown clay layer with a few angular gravels (0.5–1.5 cm). The well-preserved sediment sequence was sectioned at 2 cm intervals and labeled as LDP-1–LDP-18. All the samples were frozen in cold storage prior to analysis.

3.2 Analytical methods

Each sample was air-dried in a clean laboratory and homogenized with a mortar and pestle, and then sieved through a 200-mesh sieve. For determination of element Cu, Zn, Pb, Co, Ni, P and Cr content, about 0.25 g of each powder sample was taken, precisely weighed, digested by multi-acids, and then determined using inductively coupled plasma-atomic emission spectrometry (ICP-AES). Concentrations of Se were determined by atomic fluorescent hydrogenation (AFS). Precision and accuracy of our results were monitored by analyzing sediment standard reference materials (GBW-7301a and GBW-7408) in every batch of analysis. The analyzed results for the trace elements are within ±0.5% of the reference values. The analyzed values of Cu, Zn, Pb, Co, Ni, P, Cr and Se are listed in Table 1. The concentrations of element SiO_2, Al_2O_3, Fe_2O_3, K_2O, Na_2O, CaO, MgO, Sr and Ba were analyzed and published in Yang et al. (2018).

Table 1 The analyzed values of Cu, Zn, Pb, Co, Ni, P, Cr and Se in the palaeo-notch sediment profile LDP

Sample ID	Depth/cm	Cu/($\mu g \cdot g^{-1}$)	Zn/($\mu g \cdot g^{-1}$)	Pb/($\mu g \cdot g^{-1}$)	Co/($\mu g \cdot g^{-1}$)	Ni/($\mu g \cdot g^{-1}$)	P/($\mu g \cdot g^{-1}$)	Cr/($\mu g \cdot g^{-1}$)	Se/($\mu g \cdot g^{-1}$)
LDP-1	2	8.55	40.27	20.90	10.68	15.76	566.02	35.71	0.34
LDP-2	4	10.39	45.32	20.92	12.59	19.37	695.10	42.54	0.43
LDP-3	6	9.36	47.50	25.90	13.78	19.52	642.64	34.91	0.28
LDP-4	8	6.74	44.20	18.01	9.75	14.09	453.86	32.10	0.26
LDP-5	10	8.23	35.49	18.14	10.87	16.90	496.45	26.86	0.30
LDP-6	12	10.18	46.87	19.03	11.20	19.61	578.54	34.97	0.37
LDP-7	14	7.92	33.65	16.81	9.74	15.68	475.02	32.93	0.31
LDP-8	16	9.77	37.44	17.12	10.32	17.81	545.65	36.53	0.35
LDP-9	18	11.19	41.80	18.05	11.48	19.58	596.95	39.64	0.36
LDP-10	20	17.14	48.43	19.41	13.23	29.09	649.72	45.88	0.40
LDP-11	22	11.90	45.02	18.40	12.20	21.27	632.71	39.90	0.38
LDP-12	24	9.49	34.73	15.45	9.26	15.92	528.70	32.94	0.27
LDP-13	26	10.43	35.53	16.07	9.68	16.66	540.52	34.45	0.24
LDP-14	28	10.37	36.62	16.05	10.01	16.75	563.01	36.05	0.25
LDP-15	30	10.50	35.22	15.76	9.96	17.04	561.73	35.34	0.25
LDP-16	32	11.04	37.92	16.75	10.51	18.20	592.96	37.97	0.29
LDP-17	34	8.79	30.68	14.81	8.20	13.41	496.42	30.23	0.20
LDP-18	36	7.76	28.31	14.26	7.50	12.43	444.07	25.91	0.15

For grain size analysis, ~ 0.5 g of fully dispersed dry sample was taken, 10 mL of H_2O_2 solution (10%) was added, and the mixture was heated to 100℃ for 30 min to remove organic matter. Then 10 mL of HCl solution (10%) was added to remove carbonate and shell fragments. Finally, all the samples were fully dispersed by adding 10 mL $(NaPO_3)_6$ (10%) and treated by ultrasonic for 15 min before measurement. The grain size was analyzed using the LS230 laser diffraction particle size analyzer (Beckman Coulter, Inc.). We also analyzed the sensitive components, which reflect the difference at the same grain size interval of the grain size contents of different samples. We calculated the standard deviations of the grain size contents for all samples and the sensitive components of grain size were obtained using the grain size-standard deviation variation curve.

Total nitrogen (TN) and total carbon (TC) were determined by NCSH elemental analyser (vario EL) with an error of less than 1%. Blank samples and standard with known elemental composition (sulfanilamide) were used for quality assurance. Total organic carbon (TOC), C/N atomic ratios and $\delta^{13}C$ values measured during AMS ^{14}C dating were reported by Yang et al. (2018). In this study, TC and TOC contents were used to calculate carbonates ($CaCO_3$= (TC−TOC) × 8.333) (Müller et al., 2012).

The dry bulk density (*DBD*) of the sediments was measured using a density determination kit for Excellence XP/XS analytical balances (Mettler-Toledo AG, Laboratory & Weighing Technologies, Switzerland).

According to previous studies (Choudhary et al., 2010; Ishiwatari et al., 2005), the following equation was used to estimate the palaeoproductivity (*PP*: $g\ C \cdot m^{-2} \cdot a^{-1}$),

$$PP=(\%TOC \times DBD)/(0.0030 \times S^{0.3}), \quad \text{Equation (1)}$$

where *DBD* is the dry bulk density ($g \cdot cm^{-3}$) of the sample and *S* is the sedimentation rate ($cm \cdot ka^{-1}$). The sedimentation rate used in this study is calculated from the linear interpolation of dating results.

As for the calculation of the relative content of allochthonous and autochthonous organic matters, Colman et al. (1996) estimated the terrigenous organic carbon content in Lake Baikal sediments based on the assumption that C/N atomic ratio is 7.4 for algal organic matter and 22 for terrestrial plant organic matter. A similar assumption was made by Ishiwatari et al. (2005) to estimate the percent of autochthonous organic carbon. We also used a similar mixing model in this study. We adopted the average C/N atomic ratios (43) of four common tundra plants near our sampling site (Yuan et al., 2010) as the C/N atomic ratio for allochthonous organic matter. As we did not find any papers about C/N atomic ratios for lacustrine algae near our sampling site, we used the average C/N atomic ratio for lacustrine algae (Meyers, 1994), which is widely used in other studies. Based on this assumption, the compositions of autochthonous and allochthonous sources could be determined more accurately.

4 Results and discussion

4.1 Chronology and sedimentology

The chronology of sediment profile LDP was established using AMS ^{14}C dating techniques. Six bulk sediment samples were selected for AMS ^{14}C dating at Center for Applied Isotope Studies, University of Georgia and one sample at the bottom was supplemented for AMS ^{14}C dating at A.E. Lalonde AMS Laboratory, University of Ottawa. Radiocarbon dates were calibrated using Clam 2.2 (Blaauw, 2010) based on IntCall13 radiocarbon age calibration curve (Reimer et al., 2013). The chronology throughout the core was created using Clam 2.2 (Blaauw, 2010) (supplementary Figure 1) and the detailed results of LDP chronology was reported by Yang et al. (2018). The temporal resolution of the sediment profile is relatively low with temporal sampling resolution of ~200 a, which may make it difficult to interpret high-resolution climate records. However, it is very difficult to find well-preserved and long time span sediment sequences during mid to late Holocene because glaciers during the Little Ice Age, the most extensive in the Holocene, destroyed large quantities of sediment sequences in Svalbard. Fortunately, palaeo-notch sediments could withstand glaciers and be well-preserved after deposition. Therefore, it is a valuable material to reconstruct past climate changes in the study area.

As the lithology of LDP has little difference throughout the entire sediment profile, we performed grain size analysis to investigate the particle size compositions at different layers. Grain size standard deviation curve of the sediment profile exhibits peak values at 33 μm and 373 μm, labeled as component 2 and 3, respectively (Figure 2). The fine fraction (<2 μm) was labeled as component 1. The variation range of component 2 is 37%–96% with a mean value of 71%, so the sediment profile is mainly composed of clayey silt. The grain size contents of component 1 and 2 show opposite trends compared with component 3, while the variations of component 1 and 2 are similar with TOC contents.

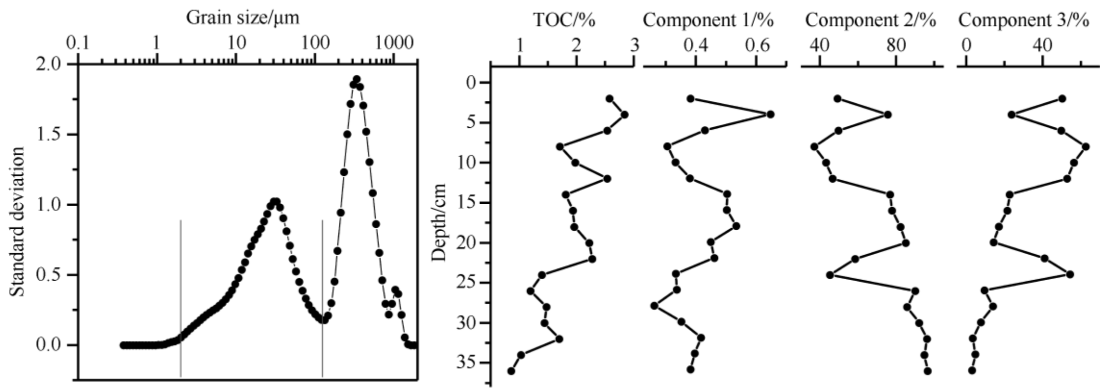

Figure 2 Grain size-standard deviation curve (left) and the variations of component 1, 2 and 3.

TOC and TN are generally considered to be a good proxy for relative organic matter content in sediments. In the sediment profile LDP, the TOC and TN contents have an increasing trend toward the surface sediment, thus the organic matter content increases towards the upper part of the sediment profile. The C/N atomic ratio is widely used to distinguish between different origins of organic matter. The C/N atomic ratios of the sediment profile LDP has very small variation range between 7.78 and 10.22, indicating a relatively stable source of organic matter.

The $CaCO_3$ content was calculated according to the formula by Müller et al. (2012), to reflect the carbonate abundance. In LDP, the $CaCO_3$ content ranges from 2.34% to 20.21% and it has a decreasing trend toward the upper part of the sediment. The vertical profile of $CaCO_3$ content shows a trend opposite to those of TOC and TN, likely due to the relative dilution of organic matter input. Yoon et al. (2006) reconstructed postglacial palaeoproductivity in Long Lake, King George Island, West Antarctica and got similar results with us.

The P concentrations in the sediment profile LDP varies from 444.07 to 695.09 $mg \cdot kg^{-1}$, with an average of 558.59 $mg \cdot kg^{-1}$. P is generally regarded as the limiting nutrient in lakes and higher P loads may lead to enhanced primary productivity (Schindler, 1978). As expected, the P concentration shows good agreement with TOC content in the palaeo-notch sediment profile.

Based on the geochemical characteristics, temporal changes of these proxies can be divided into three periods (Figure 3). Period I is characterized by relatively low TOC, TN and P contents, high $CaCO_3$ contents and dry bulk density, and thus less organic matter input. Between period I and period II is a trough of TOC and TN content, likely related to the “4.2 ka” cooling event (Roland et al., 2014). Afterward, the TOC, TN and P contents rise and peak around 3700 BP during period II and then decrease to another trough around 2800 BP, also a great cooling period (Plunkett and Swindles, 2008). During period II, CaCO3 content and dry bulk density all show a decreasing trend while the C/N atomic ratio has an opposite variation trend, indicating increasing input of allochthonous organic matter. During period III, overall, the changes of TOC, TN and P contents show an increasing trend upwards; and the C/N atomic ratio has a sharp decrease, indicating a rapid decrease in the input of allochthonous organic matter.

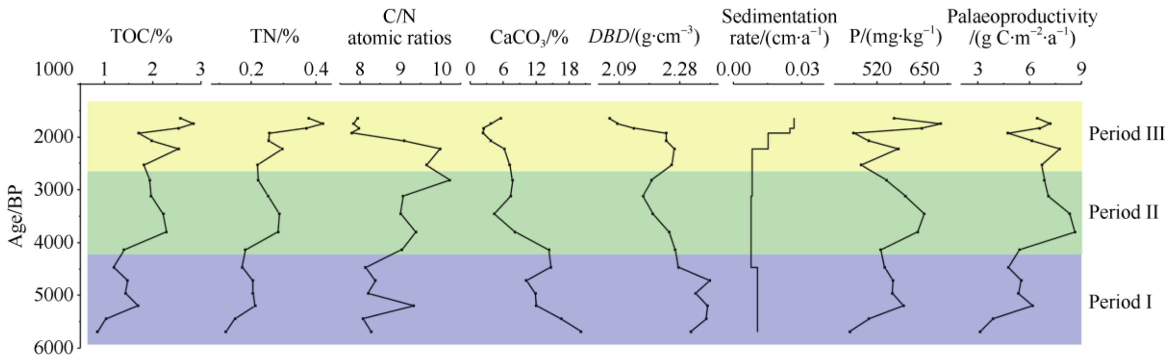

Figure 3 Down-core variation profiles of total organic carbon (TOC), total nitrogen (TN), C/N atomic ratios, the contents of $CaCO_3$, dry bulk density (*DBD*), sedimentation rate, the contents of P, and palaeoproductivity for the LDP sediment sequence.

4.2 Sources of organic matter

The organic matter preserved in the lacustrine sediments could provide important information about lake palaeoenvironment and climate change (Vreca and Muri, 2006). In LDP, the C/N and Sr/Ba atomic ratios indicate that the palaeo-notch sediment was accumulated in a lacustrine environment (Yang et al., 2018). The C/N atomic ratios of nearly all samples are lower than 10, thus the organic matter are mainly derived from lacustrine algae (Meyers, 1994). In addition, both $\delta^{13}C$ and C/N atomic ratio can be used to distinguish the origin of organic matter (Meyers, 1994). Here $\delta^{13}C$ values measured during AMS ^{14}C dating and corresponding C/N atomic ratios in the palaeo-notch sediment, as well as $\delta^{13}C$ values and C/N atomic ratios of four different lakes in the Arctic region, are plotted in $\delta^{13}C$ and C/N space (Figure 4). Nearly all the values of the palaeo-notch sediment fall in the area of lake algae, further confirming that lake algae is the major contributor to organic matter in the sediments. Thus the sediments in the palaeo-notch are accumulated in a lacustrine environment, consistent with the results from the Antarctic (Sun et al., 2005).

The organic matter in the sediment profile LDP comes from both allochthonous and autochthonous sources, and the proportion varies in LDP different periods. The autochthonous source is mainly derived from lake algae, while the allochthonous part of the sediment is mainly derived from the weathering materials around the sampling site. In addition, organic matter from surrounding vegetation could also be transported to the palaeo-notch. C/N atomic ratio is generally assumed to be an index of the contribution of terrestrial organic matter relative to algae-derived organic matter (Ishiwatari et al., 2005). In order to estimate the relative organic matter contribution from allochthonous and autochthonous sources in LDP, we also used a mixing model. Yuan et al. (2010) determined the C/N atomic ratios of four common tundra plants near our

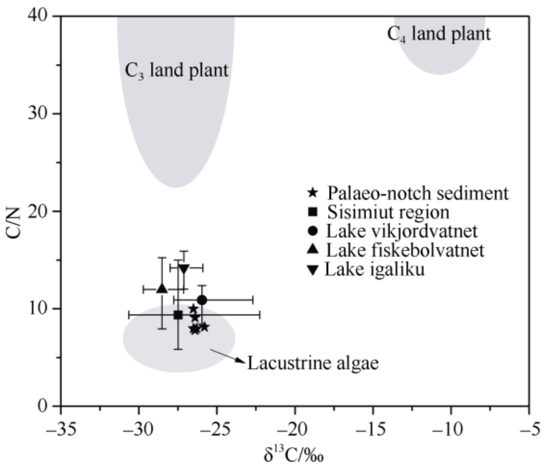

Figure 4 C/N atomic ratios and δ^{13}C for lacustrine algae, C_3 land plants, C_4 land plants and sediments in the palaeo-notch; δ^{13}C values and C/N atomic ratios from a small fresh lake near Sisimiut in south-west Greenland (Leng et al., 2012), Lake Vikjordvatnet and Lake Fiskebolvatnet in the Lofoten Island, northern Norway (Balascio and Bradley, 2012), and Lake Igaliku in south Greenland (Massa et al., 2012) are also plotted in the figure for comparison.

sampling site (with an average of 43) and thus we assumed a C/N atomic ratio of 43 for allochthonous organic matter. As the C/N atomic ratio of lacustrine algae ranges from 4 to 10, we assumed a C/N atomic ratio of 7 for autochthonous organic matter. Based on the above assumption, we calculated the relative content of allochthonous and autochthonous organic matters (Figure 5a). The autochthonous organic matter ranges from 91% to 98% of TOC, it is the major contributor of the sediment organic matter, and the temporal variations of autochthonous organic carbon (OC) are very similar to that of sediment TOC (Figure 5b).

4.3 Geochemical characteristics

The element contents in sediments are influenced by various factors and the geological explanations for any single element are complex, however, an assemblage of elements could be used to indicate different material sources (Liu et al., 2006; Sun and Xie, 2001; Sun et al., 2000). "Bio-elements" have been utilized as important geochemical markers in the Antarctic (Sun et al., 2000) and South China Sea (Liu et al., 2006) to indicate the influence of seabird. We performed *R*-mode cluster analysis with scaled data of 19 proxies, and the results showed that TOC,

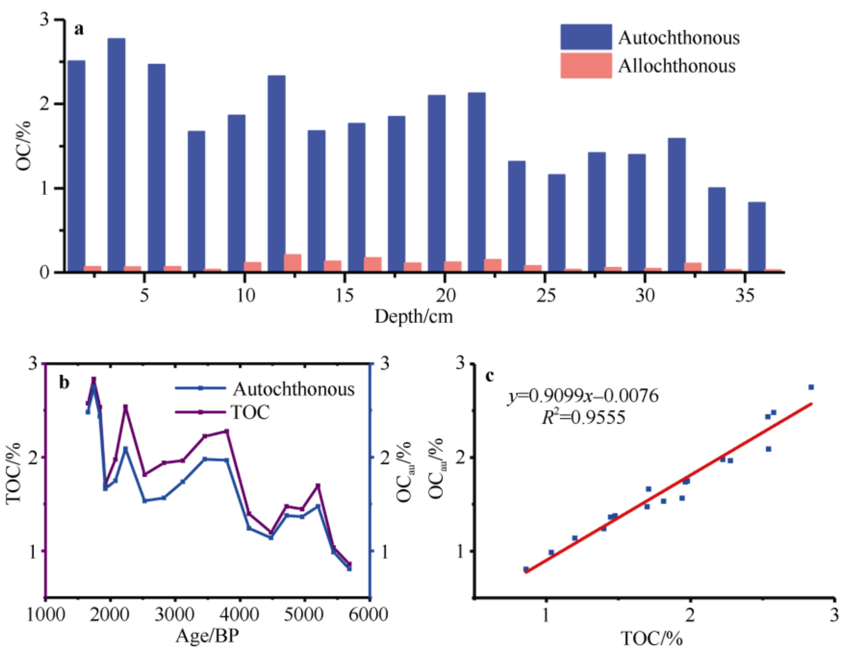

Figure 5 **a**, Variations in allochthonous and autochthonous organic carbon (OC) estimated using C/N atomic ratio for sediment profile LDP from Blomstrandhalvøya; **b**, Temporal variations in total organic carbon (TOC) and autochthonous organic carbon (OC); **c**, Correlation between TOC and autochthonous OC.

TN, Se, Pb, Zn, Ba, Co, Al_2O_3, Fe_2O_3 and K_2O are clustered into one group (Figure 6), indicating a similar variation trend. Then we performed principle component analysis (PCA) on the major and trace elements contents of the palaeo-notch sediment LDP. PC1, characterized by TOC, TN, Se, P, Pb, Zn, Ba, Co, Al_2O_3, Fe_2O_3 and K_2O, is the main controlling factor in the element contents. Pearson correlation analyses on these elements were performed and the results are listed in Table 2.

The material sources of the palaeo-notch sediment are mainly from weathering products (Yang et al., 2018) and organic matter derived from lake algae. Al_2O_3, Fe_2O_3 and

Table 2 Correlation coefficients among the elements in the palaeo-notch sediment profile LDP

	TOC	TN	Pb	Se	P	Zn	Co	Ba	K_2O	Fe_2O_3	Al_2O_3
TOC	1.00										
TN	0.95*	1.00									
Pb	0.84*	0.89*	1.00								
Se	0.86*	0.73*	0.52	1.00							
P	0.70*	0.70*	0.63*	0.72*	1.00						
Zn	0.83*	0.79*	0.78*	0.75*	0.73*	1.00					
Co	0.85*	0.81*	0.85*	0.77*	0.85*	0.88*	1.00				
Ba	0.89*	0.81*	0.81*	0.78*	0.53	0.83*	0.86*	1.00			
K_2O	0.91*	0.82*	0.78*	0.87*	0.76*	0.89*	0.94*	0.94*	1.00		
Fe_2O_3	0.94*	0.93*	0.85*	0.84*	0.86*	0.87*	0.95*	0.85*	0.94*	1.00	
Al_2O_3	0.90*	0.84*	0.78*	0.87*	0.76*	0.88*	0.95*	0.93*	0.98*	0.95*	1.00

Note: * Significant at the 0.01 level (2-tailed).

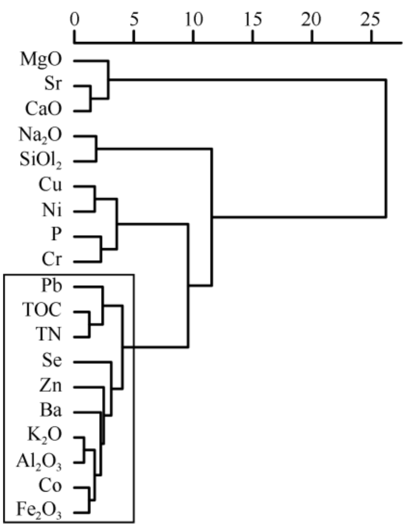

Figure 6 *R*-mode cluster analysis result for the chemical elements in the palaeo-notch sediment profile LDP.

K_2O are apparently related to chemical weathering. In addition, primary productivity controls the enrichment of most of the metals in sediments (Das et al., 2008). The levels of elements in PC1 are highly correlated with TOC and TN contents (Table 2); thus, PC1 very likely represents the total organic matter input. This is further confirmed by the similar profiles of TOC and PC1 factor score (Figure 7). As discussed above, the organic matter in the palaeo-notch sediment is mainly derived from lake algae, therefore, PC1 factor score could be the proxy for palaeoproductivity in Ny-Ålesund.

4.4 Palaeoproductivity

Estimation of variations in primary palaeoproductivity in Svalbard is important for understanding the ecological response to climate change. In this study, the palaeoproductivity was estimated according to Equation 1. However, this equation is based upon total organic carbon input, not autochthonous input. In order to better evaluate

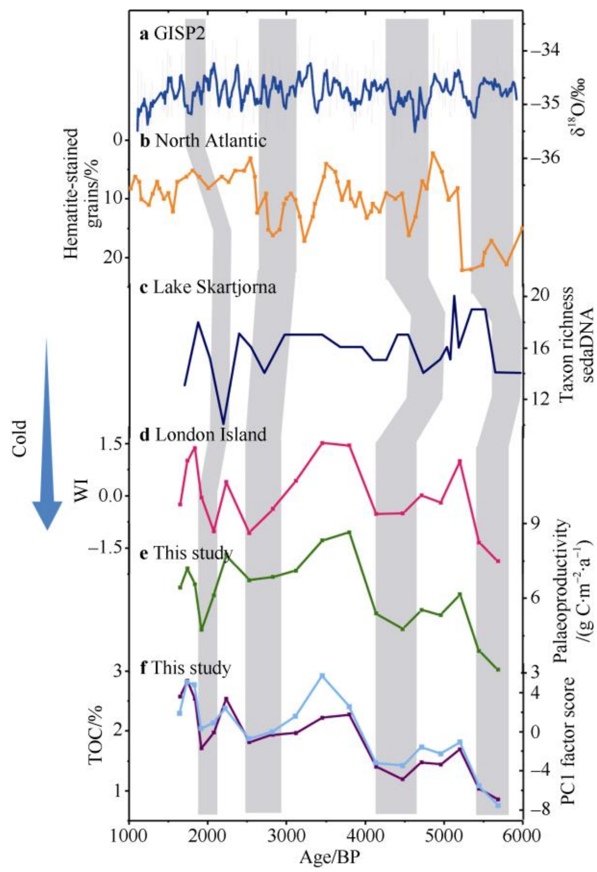

Figure 7 Comparisons between palaeoproductivity on the Blomstrandhalvøya and climatic records. **a**, The $\delta^{18}O$ profile of Greenland Ice Core GISP2 (Johnsen et al., 1997); **b**, The content of hematite-stained grains in North Atlantic sediment (Bond et al., 1997); **c**, Sedadna taxon richness records from Lake Skartjøma, Svalbard, which is used to reconstruct past vegetation changes (Alsos et al., 2016); **d**, Climatic records reconstructed through weathering intensity (WI) on the Blomstrandhalvøya, Svalbard (Yang et al., 2018); **e**, Reconstructed palaeoproductivity in palaeo-notch sediment LDP; **f**, The TOC content and PC1 factor score of sediment profile LDP. The shading area marks the cold periods.

palaeoproductivity of autochthonous organic matter input, we recalculated palaeoproductivity using the autochthonous organic matter content (Figure 3).

As shown in Figure 3, the palaeoproductivity is relatively low (3–6 g $C\cdot m^{-2}\cdot a^{-1}$) prior to 4200 BP, begins to increase thereafter, and peaks (~8.6 g $C\cdot m^{-2}\cdot a^{-1}$) around 3500 BP. Then the palaeoproductivity begins to decrease to about 6 g $C\cdot m^{-2}\cdot a^{-1}$ around 2800 BP, probably corresponding to the cold event during this period. After that, the palaeoproductivity has a slight increase and stays at a relatively stable level except the valley around 1900 BP.

TOC and TN are also extensively used as a proxy for palaeoproductivity (Arsairai et al., 2016; Prokopenko and Williams, 2004). Higher productivity is characterized by elevated organic matter content. According to the estimation of organic matter sources, the TOC content in the palaeo-notch sediment is mostly derived from in-lake algae and the variations of TOC and autochthonous OC are very similar with each other. Thus the TOC content is a good indicator for palaeoproductivity in this palaeo-notch sediment profile. Furthermore, many studies have successfully used P content to reconstruct lake productivity (Hiriart-Baer et al., 2011; Brezonik and Engstrom, 1998). Excessive P loads could promote increase in primary productivity (Liu et al., 2010; Schindler, 1978). In LDP, the variation profiles of PC1 factor score, P and TOC contents are consistent with that of the estimated palaeoproductivity, providing a further support for the reconstructed palaeoproductivity in Svalbard.

4.5 Palaeoproductivity and its response to climate change

Lacustrine sediments are ideal archives for study of palaeoclimatic and palaeoenvironmental changes, and lake palaeoproductivity is an important proxy to study the evolution of lake ecosystems. Generally, palaeoproductivity is closely related to climate change, it increases during warmer periods (Prasad et al., 2016; Jiang et al., 2011), and climate changes could leave “fingerprints” in organic matter of sediments. In this study, we reconstructed the palaeoproductivity variations in Svalbard during mid to late Holocene and compared it with the sedaDNA records, which was used to reflect past vegetation changes in the Arctic (Figure 7), from Lake Skartjørna, Svalbard (Alsos et al., 2016). The good agreement between our reconstructed palaeoproductivity and the sedaDNA records confirms the robustness of our chronology and the validity of our reconstructed palaeoproductivity.

In order to better understand the climate-ecosystem dynamics in the Arctic, we investigated the relationships between the reconstructed palaeoproductivity on the Blomstrandhalvøya and climate changes from surrounding regions (Figure 7).

According to the previous description of the palaeo-notch formation process (Yang et al., 2018), this palaeo-notch started to receive deposit no later than 5700 BP during a very cold period. This cold period is recorded in Greenland Ice Core (GISP2) $\delta^{18}O$ profile (Johnsen et al., 1997) corresponding to the ice rafting event in North Atlantic Ocean (Bond et al., 1997). In addition, the cold climate conditions terminate the Holocene thermal maximum inferred from proglacial lake sediment in Scoresby Sund region (Larsen et al., 2012; Funder, 1978). Thus the cold climate conditions during this period promoted the formation of catchment around the palaeo-notch (Yang et al., 2018). The sediment accumulated at the beginning is characterized by high $CaCO_3$ content and low TOC content, likely caused by relatively high weathering product input and low organic matter input. Climate record from Lake Skartjørna, Svalbard also shows a decline in LOI values around 5500 BP (Alsos et al., 2016). Moreover, the low value of C/N atomic ratios indicates that organic matter in the sediment is mainly derived from autochthonous sources. The low palaeoproductivity reconstructed in our record and the low sedaDNA taxon richness from Lake Skartjørna are likely a response to the cold climate conditions during this period.

TOC, PC1 factor score and the reconstructed palaeoproductivity start to increase after 5700 BP, coincident with the decrease in $CaCO_3$ content (Figure 3); this indicates an increasing organic matter content and likely warm climate conditions. From 5300 BP to 4600 BP, according to the $\delta^{18}O$ profile of GISP2 in Greenland and the content of hematite-stained grains in North Atlantic sediment, the climate is relatively warm. However, the warm climate condition was interrupted by the “4.2 ka” cooling event (Roland et al., 2014; Bond et al., 1997; Johnsen et al., 1997), in line with climate records reconstructed on the Blomstrandhalvøya. Correspondingly, the TOC and TN contents as well as palaeoproductivity in LDP all fall into a valley around 4200 BP, while the $CaCO_3$ content shows a small peak. This is consistent with the low sedaDNA taxon richness from Lake Skartjørna, Svalbard (Alsos et al., 2016).

After the “4.2 ka” cooling event, the palaeoproductivity increases rapidly and peaks around 3500 BP. The increase in TOC and TN content and decrease in $CaCO_3$ content reflect a rise in the content of organic matter in the palaeo-notch sediment. The C/N atomic ratios show a steady increase from 4200 BP to 2800 BP, indicating a gradual rise in terrestrial organic matter input. Besides, the variation of palaeoproductivity and PC1 factor score is consistent with climate change records on the Blomstrandhalvøya; the climate records in Greenland and North Atlantic also suggest a relatively warm episode during this period. However, the palaeoproductivity drops to another valley around 2600 BP, together with rapid decrease in sedaDNA taxon richness from Lake Skartjørna (Alsos et al., 2016), which coincide with the 2800 BP cooling event, well-documented in several sites from

Greenland and North Atlantic regions (Balascio et al., 2015; Bond et al., 1997). The response of the palaeoproductivity to climate changes is synchronous (Figure 7).

The climate is relatively warm from 2600 BP to 1600 BP based on the climate records from Greenland, North Atlantic and Svalbard (Yang et al., 2018; Bond et al., 2001; Johnsen et al., 1997). Correspondingly, the palaeo-productivity fluctuates around a relatively high level and the TOC content also shows an upward trend except an interruption around 1900 BP. During this interruption, the sedaDNA taxon richness from Lake Skartjørna dives to a very low level (Alsos et al., 2016). This interruption is also recorded in Greenland Ice Core (GISP2) during the corresponding period (Johnsen et al., 1997), and it might be related to a cooling event. In addition, the content of hematite-stained grains in North Atlantic sediment increased (Bond et al., 1997) and Bregne ice cap in East Greenland expanded ~1900 BP (Levy et al., 2014). Research on hydroclimate variability of High Arctic Svalbard also revealed an abrupt shift to colder conditions around 1800 BP (Balascio et al., 2016). The palaeo-lake was destroyed due to high water level in the pond or other external reasons around 1600 BP, the sediments in front of the palaeo-notch was gradually eroded and only those in the palaeo-notch were well preserved (Yang et al., 2018). Therefore, there are no records of palaeoproductivity changes in this palaeo-notch after 1600 BP.

The good agreement between palaeoproductivity changes on the Blomstrandhalvøya and palaeoclimatic records from the surrounding regions suggests that palaeoproductivity may be mainly driven by climate change in the Arctic. The palaeoproductivity increases during warm periods and decreases during cold periods. Similar observations were reported in both high altitude Tso Moriri Lake, India (Prasad et al., 2016) and Long Lake, King George Island, West Antarctica (Yoon et al., 2006). Moreover, the interruptions (cold periods) observed in the reconstructed palaeoproductivity records suggest that lake ecosystem is very sensitive to climatic and environmental changes in the Arctic.

5 Conclusions

Palaeo-notch sediment is a reliable proxy material for the study of palaeoclimate and palaeoenvironment. The C/N atomic ratios and carbon isotope results of the palaeo-notch sediment indicate that the organic matter is mainly derived from lacustrine algae. The estimation of relative organic matter contribution using C/N atomic ratios suggests that ~91%–98% of organic matter comes from autochthonous sources. The palaeoproductivity on the Blomstrandhalvøya was reconstructed using multiple geochemical proxies, and its changes are closely linked to climatic records from the surrounding regions. When the climate is warm, the palaeoproductivity increases, and vice versa. Furthermore, several interruptions in the palaeoproductivity variation profiles are likely linked to the well-known cooling periods around 1900 BP, 2800 BP and 4200 BP. The palaeo-productivity changes on the Blomstrandhalvøya are mainly driven by climate change and this study is helpful in understanding climate-ecosystem dynamics in the Arctic.

Acknowledgments The research was supported by Chinese Polar Environment Comprehensive Investigation & Assessment Programs (Grant nos. CHINARE2017-02-01, CHINARE2017-04-04). Samples information and data were issued by the Resource-sharing Platform of Polar Samples (http://birds.chinare.org.cn) maintained by Polar Research Institute of China (PRIC) and Chinese National Arctic & Antarctic Data Center (CN-NADC). We thank the Chinese Arctic and Antarctic Administration and PRIC for logistical support in field.

References

Alsos I G, Sjögren P, Edwards M E, et al. 2016. Sedimentary ancient DNA from Lake Skartjørna, Svalbard: Assessing the resilience of Arctic flora to Holocene climate change. The Holocene, 26(4): 627-642.

Arsairai B, Wannakomol A, Feng Q, et al. 2016. Paleoproductivity and paleoredox condition of the Huai Hin Lat Formation in northeastern Thailand. J Earth Sci, 27(3): 350-364.

Balascio N L, Bradley R S. 2012. Evaluating Holocene climate change in northern Norway using sediment records from two contrasting lake systems. J Paleolimnol, 48(1): 259-273.

Balascio N L, D'Andrea W J, Bradley R S. 2015. Glacier response to North Atlantic climate variability during the Holocene. Clim Past, 11(3): 1587-1598.

Balascio N L, D'Andrea W J, Gjerde M, et al. 2016. Hydroclimate variability of High Arctic Svalbard during the Holocene inferred from hydrogen isotopes of leaf waxes. Quat Sci Rev, 183: 177-187.

Birks H J B, Jones V J, Rose N L. 2004. Recent environmental change and atmospheric contamination on Svalbard as recorded in lake sediments—an introduction. J Paleolimnol, 31(4): 403-410.

Blaauw M. 2010. Methods and code for 'classical' age-modelling of radiocarbon sequences. Quat Geochronol, 5(5): 512-518.

Bond G, Kromer B, Beer J, et al. 2001. Persistent solar influence on North Atlantic climate during the Holocene. Science, 294(5549): 2130-2136.

Bond G, Showers W, Cheseby M, et al. 1997. A pervasive millennial-scale cycle in North Atlantic Holocene and glacial climates. Science, 278(5341): 1257-1266.

Brezonik P L, Engstrom D R. 1998. Modern and historic accumulation rates of phosphorus in Lake Okeechobee, Florida. J Paleolimnol, 20(1): 31-46.

Choudhary P, Routh J, Chakrapani G J. 2010. Organic geochemical record of increased productivity in Lake Naukuchiyatal, Kumaun Himalayas, India. Environ Earth Sci, 60(4): 837-843.

Cohen J, Screen J A, Furtado J C, et al. 2014. Recent Arctic amplification and extreme mid-latitude weather. Nat Geosci, 7(9): 627-637.

Colman S M, Jones G A, Rubin M, et al. 1996. AMS radiocarbon analyses from Lake Baikal, Siberia: Challanges of dating sediments from a large, oligotrophic lake. Quat Sci Rev, 15(7): 669-684.

Das S K, Routh J, Roychoudhury A N, et al. 2008. Major and trace element geochemistry in Zeekoevlei, South Africa: a lacustrine record of present and past processes. Appl Geochem, 23(8): 2496-2511.

Forman S, Lubinski D, Ingólfsson Ó, et al. 2004. A review of postglacial emergence on Svalbard, Franz Josef Land and Novaya Zemlya, northern Eurasia. Quat Sci Rev, 23(11): 1391-1434.

Funder S. 1978. Holocene stratigraphy and vegetation history in the Scoresby Sund area, East Greenland. Grønlands Geologiska Undersøgelse Bulletin, 129: 1-76.

Gajewski K. 2015. Quantitative reconstruction of Holocene temperatures across the Canadian Arctic and Greenland. Glob Planet Change, 128: 14-23.

Hiriart-Baer V P, Milne J E, Marvin C H. 2011. Temporal trends in phosphorus and lacustrine productivity in Lake Simcoe inferred from lake sediment. J Great Lakes Res, 37(4): 764-771.

Holland M M, Bitz C M, Tremblay B. 2006. Future abrupt reductions in the summer Arctic sea ice. Geophys Res Lett, 33(23): L23503.

Ishiwatari R, Yamamoto S, Uemura H. 2005. Lipid and lignin/cutin compounds in Lake Baikal sediments over the last 37 kyr: implications for glacial-interglacial palaeoenvironmental change. Org Geochem, 36(3): 327-347.

Jiang S, Liu X, Sun J, et al. 2011. A multi-proxy sediment record of late Holocene and recent climate change from a lake near Ny-Ålesund, Svalbard. Boreas, 40(3): 468-480.

Johnsen S J, Clausen H B, Dansgaard W, et al. 1997. The $\delta^{18}O$ record along the Greenland Ice Core Project deep ice core and the problem of possible Eemian climatic instability. J Geophys Res, 102(C12): 26397-26410.

Kołaczek P, Mirosław-Grabowska J, Karpińska-Kołaczek M, et al. 2015. Regional and local changes inferred from lacustrine organic matter deposited between the Late Glacial and mid-Holocene in the Skaliska Basin (north-eastern Poland). Quatern Int, 388: 51-63.

Landvik J Y, Bondevik S, Elverhøi A, et al. 1998. The last glacial maximum of Svalbard and the Barents Sea area: ice sheet extent and configuration. Quat Sci Rev, 17(1): 43-75.

Larsen D J, Miller G H, Geirsdóttir Á, et al. 2012. Non-linear Holocene climate evolution in the North Atlantic: a high-resolution, multi-proxy record of glacier activity and environmental change from Hvítárvatn, central Iceland. Quat Sci Rev, 39: 14-25.

Leng M J, Wagner B, Anderson N J, et al. 2012. Deglaciation and catchment ontogeny in coastal south-west Greenland: implications for terrestrial and aquatic carbon cycling. J Quat Sci, 27(6): 575-584.

Levy L B, Kelly M A, Lowell T V, et al. 2014. Holocene fluctuations of Bregne ice cap, Scoresby Sund, East Greenland: a proxy for climate along the Greenland Ice Sheet margin. Quat Sci Rev, 92: 357-368.

Liu E, Shen J, Zhang E, et al. 2010. A geochemical record of recent anthropogenic nutrient loading and enhanced productivity in Lake Nansihu, China. J Paleolimnol, 44(1): 15-24.

Liu X, Zhao S, Sun L, et al. 2006. Geochemical evidence for the variation of historical seabird population on Dongdao Island of the South China Sea. J Paleolimnol, 36(3): 259-279.

López-Moreno J I, Boike J, Sanchez-Lorenzo A, et al. 2016. Impact of climate warming on snow processes in Ny-Ålesund, a polar maritime site at Svalbard. Glob Planet Change, 146: 10-21.

Mangerud J, Bolstad M, Elgersma A, et al. 1992. The last glacial maximum on Spitsbergen, Svalbard. Quat Res, 38(1): 1-31.

Mangerud J, Landvik J Y. 2007. Younger Dryas cirque glaciers in western Spitsbergen: smaller than during the Little Ice Age. Boreas, 36(3): 278-285.

Massa C, Bichet V, Gauthier É, et al. 2012. A 2500 year record of natural and anthropogenic soil erosion in South Greenland. Quat Sci Rev, 32: 119-130.

Meyers P A. 1994. Preservation of elemental and isotopic source identification of sedimentary organic matter. Chem Geol, 114(3-4): 289-302.

Meyers P A, Ishiwatari R. 1993. Lacustrine organic geochemistry—an overview of indicators of organic matter sources and diagenesis in lake sediments. Org Geochem, 20(7): 867-900.

Miccadei E, Piacentini T, Berti C. 2016. Geomorphological features of the Kongsfjorden area: Ny-Ålesund, Blomstrandøya (NW Svalbard, Norway). Rendiconti Lincei, 27(1): 217-228.

Miller G H, Brigham-Grette J, Alley R B, et al. 2010. Temperature and precipitation history of the Arctic. Quat Sci Rev, 29(15-16): 1679-1715.

Müller J, Werner K, Stein R, et al. 2012. Holocene cooling culminates in sea ice oscillations in Fram Strait. Quat Sci Rev, 47: 1-14.

Plunkett G, Swindles G T. 2008. Determining the Sun's influence on Lateglacial and Holocene climates: a focus on climate response to centennial-scale solar forcing at 2800 cal. BP. Quat Sci Rev, 27(1-2): 175-184.

Prasad S, Mishra P K, Menzel P, et al. 2016. Testing the validity of productivity proxy indicators in high altitude Tso Moriri Lake, NW Himalaya (India). Palaeogeogr Palaeoclimatol Palaeoecol, 449: 421-430.

Prokopenko A A, Williams D F. 2004. Deglacial methane emission signals in the carbon isotopic record of Lake Baikal. Earth Planet Sc Lett, 218(1): 135-147.

Røthe T O, Bakke J, Vasskog K, et al. 2015. Arctic Holocene glacier fluctuations reconstructed from lake sediments at Mitrahalvøya, Spitsbergen. Quat Sci Rev, 109: 111-125.

Reimer P J, Bard E, Bayliss A, et al. 2013. Intcal13 and Marine13 Radiocarbon Age Calibration Curves 0–50,000 Years Cal Bp. Radiocarbon, 55(4): 1869-1887.

Roland T P, Caseldine C J, Charman D J, et al. 2014. Was there a '4.2 ka event' in Great Britain and Ireland? Evidence from the peatland record. Quat Sci Rev, 83: 11-27.

Schindler D W. 1978. Factors regulating phytoplankton production and standing crop in the world's freshwaters. Limnol Oceanogr, 23(3): 478-486.

Sun L, Liu X, Yin X, et al. 2005. Sediments in palaeo-notches: potential proxy records for palaeoclimatic changes in Antarctica. Palaeogeogr Palaeoclimatol Palaeoecol, 218(3): 175-193.

Sun L, Xie Z. 2001. Relics: penguin population programs. Science progress, 84(1): 31-44.

Sun L, Xie Z, Zhao J. 2000. A 3,000-year record of penguin populations. Nature, 407(6806): 858-858.

van der Bilt W G M, Bakke J, Vasskog K, et al. 2015. Reconstruction of glacier variability from lake sediments reveals dynamic Holocene climate in Svalbard. Quat Sci Rev, 126: 201-218.

Vreca P, Muri G. 2006. Changes in accumulation of organic matter and stable carbon and nitrogen isotopes in sediments of two Slovenian mountain lakes (Lake Ledvica and Lake Planina), induced by eutrophication changes. Limnol Oceanogr, 51(1, part 2): 781-790.

Yang Z, Sun L, Zhou X, et al. 2018. Mid to late Holocene climate change record in palaeo-notch sediment from London Island, Svalbard. J Earth Syst Sci, 127(4): 57.

Yang Z, Yuan L, Wang Y, et al. 2017. Holocene climate change and anthropogenic activity records in Svalbard: a unique perspective based on Chinese research from Ny-Ålesund. Adv Polar Sci, 28(2): 81-90, doi: 10.13679/j.advps.2017.2.00081.

Yoon H, Khim B, Lee K, et al. 2006. Reconstruction of postglacial paleoproductivity in Long Lake, King George Island, West Antarctica. Pol Polar Res, 27(3): 189-206.

Yuan L, Sun L, Long N, et al. 2010. Seabirds colonized Ny-Ålesund, Svalbard, Arctic ~ 9,400 years ago. Polar biol, 33(5): 683-691.

Zhang T, Wei X L, Zhang Y Q, et al. 2015. Diversity and distribution of lichen-associated fungi in the Ny-Ålesund Region (Svalbard, High Arctic) as revealed by 454 pyrosequencing. Sci Rep, 5: 14850, doi: 10.1038/srep14850.

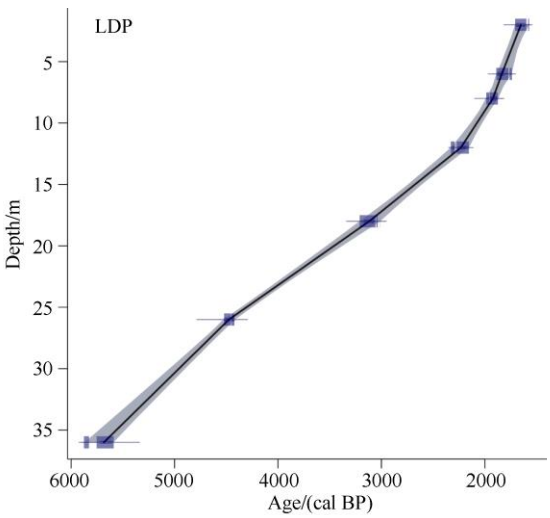

Supplementary Figure 1 The age-depth model for the sediment profile LDP based on ^{14}C dating of bulk sediments at different depths.